Journal of Industrial and Engineering Chemistry 105 (2022) 481–490

Contents lists available at ScienceDirect

Journal of Industrial and Engineering Chemistry

journal homepage: www.elsevier.com/locate/jiec

Comestible curcumin: From kitchen to polymer chemistry as a photocatalyst in metal-free ATRP of (meth)acrylates

I. Zaborniak, P. Chmielarz *

Department of Physical Chemistry, Faculty of Chemistry, Rzeszow University of Technology, Al. Powstańców Warszawy 6, 35-959 Rzeszów, Poland

ARTICLE INFO

Article history:
Received 8 September 2021
Revised 1 October 2021
Accepted 3 October 2021
Available online 9 October 2021

Keywords:
Curcumin
Visible light
Metal-free ATRP
Comestible curcumin

ABSTRACT

The article presents an application of curcumin, a widely available and cost-effective organic dye, to control visible-light mediated ATRP. A two-component photocatalytic system composed of curcumin and an amine-based electron donor activates alkyl bromide and controls radical polymerizations by a reductive quenching pathway. The polymerizations of various types of (meth)acrylates were performed under blue LED irradiation (λ_{max} = 460 nm, 5 mW cm^{-2}). The effect of electron donor type, solvent, photocatalyst and electron donor concentration, target degree of polymerization (DP_{target}) etc. on the metal-free ATRP of methyl methacrylate (MMA) and poly(ethylene glycol) methyl ether methacrylate ($OEGMA_{500}$) was systematically investigated to optimize the polymerization conditions. Moreover, comestible curcumin of four different brands available in the market as kitchen spices was used, which makes this approach economical (~0.04 € for 15 g of turmeric). In order to increase the applicability of the curcumin-based polymerization strategy, the concept was extended to the polymerization of other methacrylates – butyl methacrylate (*n*BMA), di(ethylene glycol) methyl ether methacrylate (DEGMA), 2-(dimethylamino) ethyl methacrylate (DMAEMA), and acrylates i.e. poly(ethylene glycol) methyl ether acrylate ($OEGA_{480}$), *n*-butyl acrylate (*n*BA) and 2-hydoxyethyl acrylate (HEA). In situ chain extension experiment demonstrated the preservation of chain-end functionality, enabling the facile synthesis of well-controlled copolymers.

Introduction

Light as a widely available, relatively safe and economical external stimulus has attracted much attention as an initiating factor in controlled radical polymerization techniques, e.g. atom transfer radical polymerization (ATRP) approach [1–4]. Polymers prepared by ATRP are characterized by a narrow molecular weight distribution and a controlled structure, therefore it is one of the most convenient methods to prepare precisely defined polymer structures with various architectures [5–11]. There is classical ATRP approach with high catalyst concentration and low ppm techniques controlled by chemical reducing agents, i.e. ascorbic acid [8,12,13], glucose [14], Ag^0 [15], other zerovalent metals [16,17], and thermal radical initiators [18], and external stimuli, i.e. electric current [19,20], ultrasound [21], and light [3,22,23]. Among these techniques, photoinduced ATRP provides a wide range of polymer types using a simple experimental setup, mild reaction conditions, limiting small side effects, with the possibility of adjusting the light source, and spatial and temporal control [2,24–27]. Light of various wavelengths can be effectively used in photocontrolled polymerizations, including UV [1], visible [4,28] and near infrared (NIR) [29,30] delivered by e.g. household bulbs [31], light-emitting diodes (LEDs) [32] or even sunlight [4].

Initially, the concept of photoinduced ATRP involved the use of light sources to reduce transition metal photoredox catalyst complexes, eliminating chemical reducing agents from the reaction setup. Transition metals i.e. Cu [33,34], Fe [35], Ir [36], Ru [37] provided an excellent control over light-mediated polymerization processes. However, for numerous applications such as biomedicine, biomaterials or microelectronics, metal contamination is a limiting factor in the use of ATRP as a synthetic pathway – despite the elaboration of low ppm techniques rapidly developed in recent years.

Following these obstacles, further development of the light-induced ATRP led to the elimination of metal-based catalysts from the reaction setup, that were replaced by photocatalysts (organic compounds) excited by light. Initially, 10-phenylphenothiazine (Ph-PTZ) [1,38], perylene [39,40] and diaryl dihydrophenazines [41], and recently developed oxygen-doped anthanthrene [4] have been successfully used to catalyze the polymerization of various

* Corresponding author.
E-mail address: p_chmiel@prz.edu.pl (P. Chmielarz).

https://doi.org/10.1016/j.jiec.2021.10.001
1226-086X/

monomers. Following this concept, organic dyes turned out to be efficient photocatalysts in metal-free ATRP, i.e. eosin Y [23,32,42], erythrosin B [32], fluorescein [3,23,43], 1′-diethyl-2,2′-cyanine iodide [28], methylene blue [44], Nile red and Rhodamine 6G [23]. The use of organic dyes provides low cost, they are readily available and easy to use in mediated by visible light metal-free ATRP of a wide range of monomers. Compared to ultraviolet light with a high energy (∼6 eV), visible light – a relatively safe and economical low energy ∼2 eV external resource, exhibits higher potential in synthesis and applications [43]. Polymerization mediated by visible light is considered to be a green technology.

Organic dyes participate in light-mediated ATRP through reductive quenching pathways. It means that excited state photocatalyst is unable to reduce the initiator directly, as in the oxidative quenching concept [22,32,45], and therefore the catalyst needs an electron donor to provide sufficient negative reduction potential to control the polymerization. Upon visible light photon absorption, an organic dye is converted to its excited state, followed by the generation of reductant through reversible electron transfer from an electron donor (usually trialkylamines) according to a reductive quenching pathway. A dye-based reductant participates in the dehalogenation of the initiator to form carbon-central radical species, which are responsible for the initiation of the polymerization.

A step forward to design a fully biocompatible photoinduced controlled polymerization setup is the use of a two-component photocatalytic system composed of naturally-derived and widely available components i.e. riboflavin (vitamin B_2) playing the role of a photocatalyst and ascorbic acid (vitamin C) as a mild reducing agent [26]. The use of economical and readily available compounds in ATRP mediated by light is a direction that has been strongly developed in recent years. The present work proposes the use of curcumin and comestible curcumin as a photocatalyst in the metal-free ATRP of a wide range of acrylates and methacrylates. Among the possibilities of applying visible light, this concept is also beneficial due to the use of a naturally-derived and biocompatible photocatalyst, also with a medical action, widely available in nature, and advantageous from an economic point of view through the use of cheap kitchen spices.

Curcumin is a naturally-derived yellow-orange product, which is a member of the ginger family [46]. Among its anti-cancer, antibacterial, anti-inflammatory, and antioxidant properties [47,48], curcumin has also enormous potential for the use in a photoinduced radical polymerization technique [49–52]. It is a type of multicolor photoinitiator with panchromatic light absorption. Therefore, curcumin catalyzed photopolymerization can be trigged by various wavelengths of incident light (from UV to red light), hence utilization of this type of bio-based molecules in modern polymer chemistry is highly interesting [51]. Under illumination by both ultraviolet and visible light, it can accept and lose a pair of hydrogen atoms through reduction and oxidation processes, respectively. It can be excited to a singlet state with a short life and then transform into a triplet excited state characterized by long life and high reactivity, which is a crucial feature for an efficient photoactivator in the metal-free ATRP [49]. Up to now, curcumin was extensively studied in free radical polymerization [49,51–54]. It has never been used as a photocatalyst in controlled radical polymerizations, thus it is an excellent direction for the development of naturally-derived photocatalytic systems for RDRP techniques.

Herein, visible-light mediated ATRP is presented with the two-component photocatalytic system composed of curcumin and amine-based electron donor. The polymerizations of various types of methacrylates and acrylates were performed under blue LED irradiation (λ_{max} = 460 nm, 5 mW cm^{-2}). The effects of electron donor type, solvent type, photocatalyst and electron donor concentration, target degree of polymerization (DP_{target}) etc. on metal-free ATRP of methyl methacrylate (MMA) and poly(ethylene glycol) methyl ether methacrylate ($OEGMA_{500}$) were systematically investigated to optimize the polymerization conditions. Moreover, the curcumin with laboratory purity has been substituted by comestible curcumin from of different brands available in market as kitchen spices, making this approach an economic solution (∼0.04 € for 15 g of curcuma). In addition, to increase the applicability of this curcumin-based polymerization strategy, we tried to extend it to the polymerization of other methacrylates – butyl methacrylate (*n*BMA), di(ethylene glycol) methyl ether methacrylate (DEGMA), 2-(dimethylamino)ethyl methacrylate (DMAEMA), and acrylates i.e. poly(ethylene glycol) methyl ether acrylate ($OEGA_{480}$), *n*-butyl acrylate (*n*BA) and 2-hydoxyethyl acrylate (HEA). Compared to other ATRP techniques, the proposed concept completely eliminates the transition metal from the reaction setup, and thus the need for chemical reducing agents. Instead, the environmentally friendly, cost-effective and renewable photocatalyst is used. Consequently, the proposed approach significantly reduces the number of purification steps. Considering other externally controlled ATRP techniques, e.g. electrochemically-mediated approach, no electrolyte is needed and the reaction system is greatly simplified and therefore easy to use on an industrial scale, only a simple LED light source is necessary.

Results and discussion

Effect of electron donor type, initiator to curcumin ratio, and curcumin to electron donor ratio on curcumin-catalyzed metal-free ATRP of MMA

To activate the alkyl bromide in the ATRP process, an organic catalyst as curcumin at a highly reducing state is necessary. Curcumin – a dye-based photoinitiator participates in photoinitiated ATRP through a reductive quenching pathway. Therefore, an electron donor is needed to provide electron for reduction of the dye's excited state Cur*, resulting in the formation of photocatalyst in the form of an anion radical $Cur^{\bullet -}$ that is able to reduce alkyl halide (ATRP initiator) under visible light irradiation (λ_{max} = 460 nm, 0.50 mW cm^{-2}) to produce an electron-deficient alkyl radical for chain propagation.

Tertiary amine electron donors such as triethylamine (TEA), *N*,*N*,*N*′,*N*″,*N*″-pentamethyldiethylentriamin (PMDETA), and 1,1,4,7,10,10-hexamethyltriethylenetetramine (HMTETA) with a similar structure were studied. The electrons transferred from the electron donor to curcumin reside in the tertiary nitrogen atom. The proposed reductants differ in the number of tertiary nitrogen atoms in their structure, i.e. TEA includes one, PMDETA – three, and HMTETA – four N atoms as a source of electrons. Experiments were performed in dimethylformamide (DMF), with 2-bromopropionitrile (BPN) as the initiator, targeted degree of polymerization (DP) of 300 by employing a 1/0.2 ratio of BPN/curcumin, varying the ratio of curcumin and electron donor between 1/5 to 1/30 (Table 1, entries 1–6, Figs. 1 and S2).

In the presence of TEA, a non-linear kinetic profile was observed, regardless of electron donor concentration. The monomer was rapidly consumed up to ca. 10%, then it slowed down and the dependence of $\ln([M]_0/[M])$ deviated from linearity (Fig. 1a). The use of 30-fold excess of TEA instead of 5-fold resulted in an increase of final dispersity (M_w/M_n = 1.53 vs. 1.69 for 1/5 and 1/30 $[Curcumin]_0/[Electron\ donor]_0$ molar ratio, see Table 1), and the lower MMA conversion was reached (18.5% and 11.9% for 1/5 and 1/30 of $[Curcumin]_0/[Electron\ donor]_0$ molar ratio, see Table 1). A high concentration of TEA reduced the dye's excited state faster, resulting in the formation of a curcumin-based anion radical that

Table 1
Polymerization of methyl methacrylate by curcumin catalyzed metal-free ATRP concept.[1]

Entry	Electron donor	$[BPN]_0$/ $[Curcumin]_0$	$[Curcumin]_0$/$[Electron\ donor]_0$	DP_{target}	Time (h)	Conv[2] (%)	k_p^{app}[3] (h^{-1})	$DP_{n,\ theo}$[2]	$M_{n,theo}$[4] (x10^{-3})	$M_{n,app}$[5] (x10^{-3})	M_w/M_n[5]	I_{eff}[6] (%)
1	TEA	1/0.2	1/5	300	3.5	18.5	0.057	55	5.7	70.5	1.53	8.1
2	TEA	1/0.2	1/30	300	3.5	11.9	0.039	36	3.7	63.2	1.69	5.9
3	PMDETA	1/0.2	1/5	300	3.5	15.6	0.043	47	4.9	76.3	1.51	6.5
4	PMDETA	1/0.2	1/30	300	3.5	24.5	0.075	73	7.5	66.5	1.56	11.3
5	HMTETA	1/0.2	1/5	300	3.5	23.6	0.079	71	7.3	69.6	1.56	10.4
6	HMTETA	1/0.2	1/30	300	3.5	38.4	0.124	115	11.7	64.9	1.60	18.0
7	HMTETA	1/0.4	1/30	300	3.5	35.1	0.125	105	10.7	60.5	1.61	17.6
8	HMTETA	1/0.4	1/30	600	3	30.6	0.120	184	18.5	68.1	1.53	27.2

[1]General conditions: T = room temperature; V_{tot} = 10 mL for entries 1–6, and V_{tot} = 5 mL for entries 7 and 8; $[MMA]_0/[BPN]_0/[Curcumin]_0/[Electron\ donor]_0$ = x/1/y/z; x = 300 for entries 1–7, and x = 600 for entry 8; y = 0.2 for entries 1–6, and y = 0.4 for entries 7 and 8; z = 1 for entries 1, 3 and 5, z = 6 for entries 2, 4 and 6, and z = 12 for entries 7 and 8; $[MMA]_0$ = 30% v/v; Blue light irradiation at 460 nm (5.0 mW cm^{-2}).
[2]Conversion and theoretical degree of polymerization ($DP_{n,\ theo}$) calculated according to ^{1}H NMR analysis, $DP_{n,theo} = (conv \cdot [MMA]_0)/[BPN]_0$ [55].
[3]Apparent rate constant of propagation, calculated as a slope of the curve $\ln[M]_0/[M] = f(t)$ illustrated in the Fig. 1a,c,e [21,56].
[4]$M_{n,theo} = [MMA]_0/[BPN]_0 \cdot conversion \cdot M_{MMA} + M_{BPN}$.
[5]Apparent $M_{n,app}$ and M_w/M_n were determined by DMF GPC.
[6]Initiation efficiency, $I_{eff} = (M_{n,theo}/\ M_{n,app}) \cdot 100\%$.

reduces initiator, thus provided a high amount of propagating radicals. In consequence, poor initiator deactivation is observed, results in radical–radical coupling.

In contrast to TEA, the PMDETA electron donor provides a polymerization characterized by a linear dependence of $\ln([M]_0/[M])$ on time (Fig. 1a), however, at molar ratio of $[Curcumin]_0/[Electron\ donor]_0$ = 1/5 it was less efficient than TEA, reaching 16% of MMA conversion and the final product with comparable dispersity (M_w/M_n = 1.51, Table 1, entry 3). The polymerization with PMDETA concentration at molar ratio $[Curcumin]_0/[PMDETA]_0$ = 1/30, conversely to TEA, results in higher monomer conversion (ca. 25%, Table 1, entry 4), accompanied by a much faster polymerization rate (k_p^{app} = 0.043 vs. 0.075 for 1/5 and 1/30 of $[Curcumin]_0/[Electron\ donor]_0$ molar ratio, respectively, see k_p^{app} in Table 1, entries 3 and 4), and slightly broader M_w/M_n (1.56, Table 1, entry 4, Fig. S2d). Considering the concentration of electron donor, the same behavior as PMDETA gives was observed with the use of HMTETA, namely increasing amounts of electron donor provides more efficient polymerization reflected by higher monomer consumption and the rate of polymerization (conv = 23.6 vs. 38.4, k_p^{app} = 0.079 vs. 0.124 for 1/5 and 1/30 $[Curcumin]_0/[Electron\ donor]_0$ molar ratios, respectively, see conv and k_p^{app} in Table 1, entries 5 and 6). For these first optimization sets of kinetics, it can be concluded that the number of tertiary nitrogen atoms in the chemical structure of an electron donor significantly influenced the polymerization efficiency. More nitrogen atoms provide more electrons transferred from the electron donor to curcumin, and therefore more propagating radicals are formed leading to a faster polymerization rate. Consequently, a lower concentration of tertiary amine with a higher amount of nitrogen atoms in its structure is needed to effectively reduce the photocatalyst in the excited state. The HMTETA electron donor with four N atoms as a source of electrons provides the most effective synthesis. Only reactions with PMDETA and HMTETA followed first-order kinetics and provided products with final M_w/M_n ~1.51–1.60 (Fig. S2c-h). For all the polymerizations, relatively pour agreement between theoretical and experimental molecular weight was observed, reflecting low initiation efficiency I_{eff} (~6–18%, see I_{eff} in Table 1). It is clearly visible on the non-linear M_n with the conversion plot (Fig. 1b). Initially, the molecular weight is rapidly grown followed by reaching the plateau despite the monomer is consumed. This is hypothetically caused by insufficient deactivation of initiator/propagating radicals, resulting in radical–radical coupling, and lagging establishment of the dynamic equilibrium between active and dormant species. It is also noted that molecular weights seem to approach more theoretical values in higher monomer conversion, therefore suggesting the tendency towards higher initiation efficiency as the monomer is consumed. Since the photocatalytic mediated processes of reductive dehalogenation of the initiator and propagation processes occur constantly during the polymerization, in the initial synthesis step, fast activation of the initiator causes formation of a high amount of the propagating radicals, and slow deactivation results in coupling reaction and low initiation efficiency. As the polymerization progresses and the monomer is consumed, a dynamic equilibrium between active and dormant species is established and the initiation efficiency increases.

The influence of $[BPN]_0/[Curcumin]_0$ molar ratio on polymerization course was subsequently studied at the molar ratio of curcumin and HMTETA electron donor of 1/30 (Table 1, entries 6 and 7, Fig. 1c,d). When even higher amounts of photocatalyst were employed ($[BPN]_0/[Curcumin]_0$ = 1/0.4) a similar kinetics profile emerged i.e. linear dependence of $\ln([M]_0/[M])$ on time (Fig. 2a) pointing at high livingness of the process. Relatively constant M_n throughout the polymerization (Fig. 1d and S2f,g) was also observed. As previously described, it is connected to the insufficient deactivation processes, therefore polymers reach their final M_n from the very beginning, before being deactivated. Comparable M_w/M_n of the final product and I_{eff} (M_w/M_n = 1.60 and 1.61, and I_{eff} = 18.0% and 17.6% for $[BPN]_0/[Curcumin]_0$ = 1/0.2 and 1/0.4, respectively, Table 1, entries 6 and 7) was received.

Initiator concentration was then reduced from 9.3 mM (Table 1, entry 7) to 4.7 mM (Table 1, entry 8) by increasing target degree of polymerization (see DP_{target}, Table 1, entries 7 and 8) at $[BPN]_0/[Curcumin]_0$ = 1/0.4 molar ratio. Applying the lower BPN amount results in insignificantly lower polymerization rate (k_p^{app} = 0.125 vs. 0.120 for DP_{target} = 300 and 600, respectively, see k_p^{app} in Table 1, entries 7 and 8), accordingly to usual ATRP behavior when the initiator concentration is reduced [57]. First-order kinetic was observed (Fig. 1e) and in contrast to DP_{target} = 300, M_n increased as the monomer consumed (Fig. 1f), providing the final product with lower dispersity (M_w/M_n = 1.53, Table 1, entry 8, Fig. S2g,h), and higher initiation efficiency (I_{eff} = 27.2 %, Table 1, entry 8). It can be concluded that a lower initiator loading, thus higher monomer concentration, caused faster initiator deactivation, therefore the polymer did not reach the final molecular weight in the initial step of the polymerization and grown constantly.

Effect of solvent type, initiator concertation (target degree of polymerization, DP_{target}) and initiator to curcumin ratio on curcumin-catalyzed metal-free ATRP of $OEGMA_{500}$

The proposed curcumin-based concept was also investigated to polymerize $OEGMA_{500}$ monomer, widely used in metal-free ATRP approach [25,26]. The syntheses were conducted in the reaction

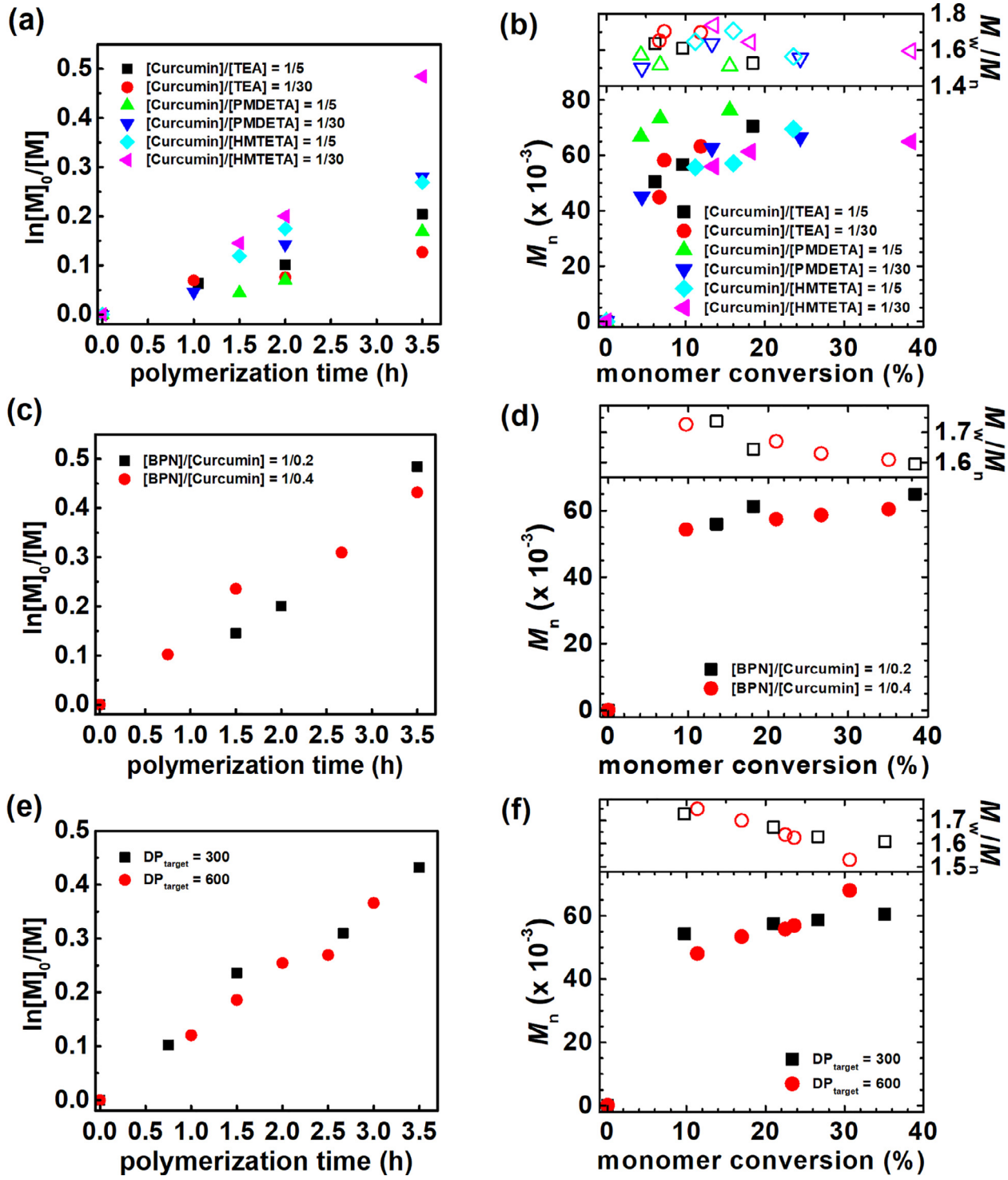

Fig. 1. Curcumin-catalyzed metal-free ATRP of MMA. (a) First-order kinetics plot of monomer conversion *vs.* polymerization time and (b) M_n and M_w/M_n *vs.* monomer conversion for experiments with various types of electron donor (Table 1, entries 1–6). (c) First-order kinetics plot of monomer conversion *vs.* polymerization time and (d) M_n and M_w/M_n vs. monomer conversion for influence study of initiator to photocatalyst molar ratio (Table 1, entries 6 and 7). (e) First-order kinetics plot of monomer conversion *vs.* polymerization time and (f) M_n and M_w/M_n vs. monomer conversion for influence study of initiator concentration (Table 1, entries 6 and 7).

setup implemented from the above-described MMA polymerization i.e. employing a 1/30 molar ratio of curcumin/HMTETA and BPN as the initiator. However, considering the different characteristics of poly(ethylene glycol)-based monomer comparing to methyl methacrylate, the scope of the proposed system was expanded by investigating the influence of different components on the polymerization course i.e. using different solvents, varying the ratio of BPN and curcumin between 1/0.4 to 1/1.6 and targeted degree of polymerization (DP) from 50 to 250 (Table 2, Figs. 2 and S3).

Investigation of the effect of different solvents on curcumin-catalyzed polymerization was conducted in polar organic solvents that dissolve the photocatalyst well, i.e. dimethyl sulfoxide (DMSO), *N*,*N*-dimethylacetamide (DMAc) and DMF, at

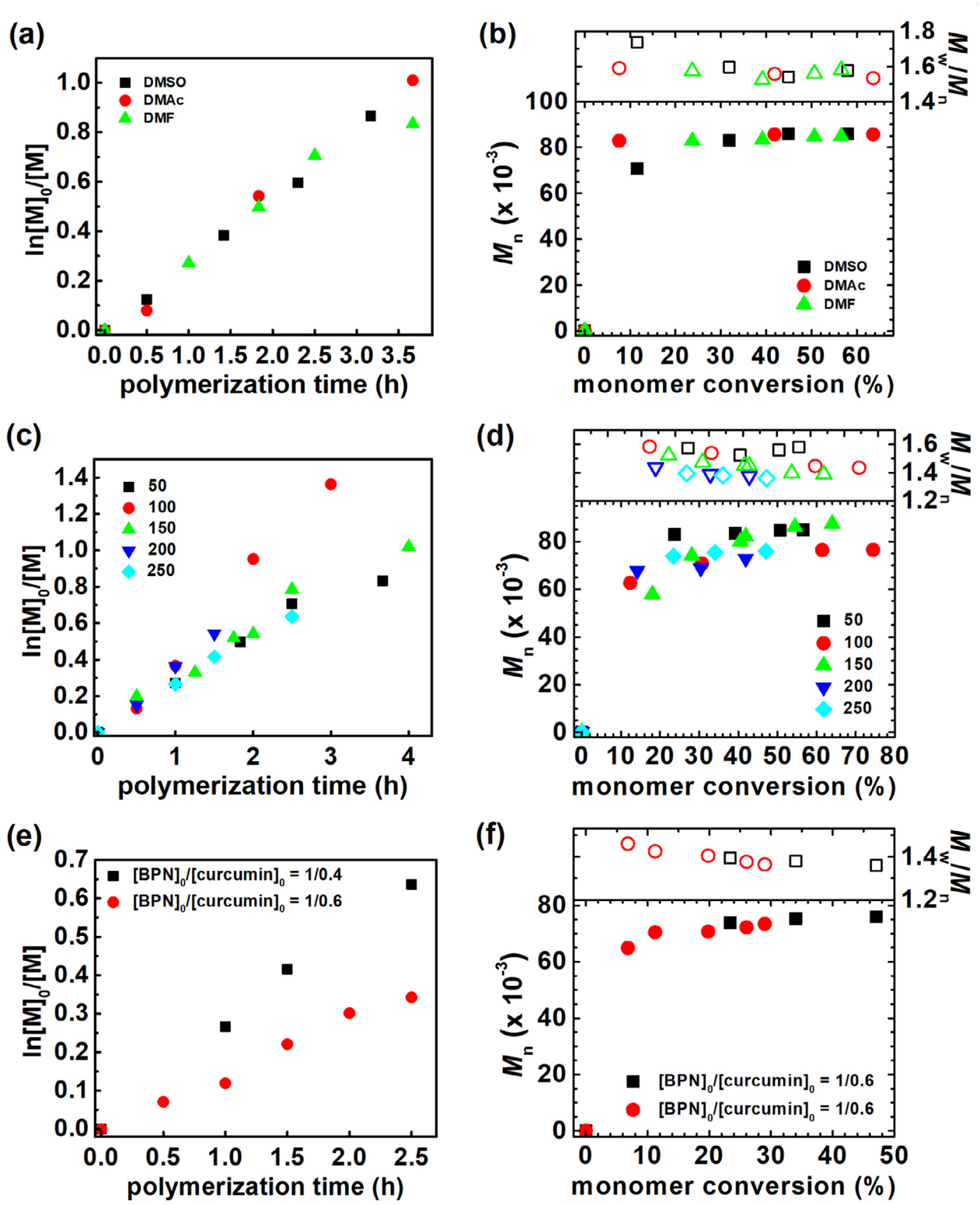

Fig. 2. Curcumin-catalyzed metal-free ATRP of $OEGMA_{500}$. (a) First-order kinetics plot of monomer conversion *vs.* polymerization time and (b) M_n and M_w/M_n *vs.* monomer conversion for influence study of solvent type (Table 2, entries 1–3). (c) First-order kinetics plot of monomer conversion *vs.* polymerization time and (d) M_n and M_w/M_n *vs.* monomer conversion for influence study of initiator concentration (Table 2, entries 3–7). (e) First-order kinetics plot of monomer conversion *vs.* polymerization time and (f) M_n and M_w/M_n *vs.* monomer conversion for influence study of initiator to curcumin ratio (Table 2, entries 7,8).

$[OEGMA_{500}]_0/[BPN]_0/[Curcumin]_0/[HMTETA]_0$ = 50/1/0.4/12 molar ratio. The experiments provided the observations that there is no significant influence on the polymerization course changing the solvent. The linear fitting curves ($\ln[M]_0/[M]$ versus time) for all syntheses suggested a constant concentration of propagating radicals during the polymerizations (Fig. 2a). Within ~ 3–4 h, ca. 60% conversion was reached regardless of the solvent used, and the apparent rate constant of propagation values calculated from the

Table 2
Polymerization of oligo(ethylene glycol methyl ether) methacrylate by curcumin-catalyzed metal-free ATRP concept.[1]

Entry	$[BPN]_0/[Curcumin]_0$	$[Curcumin]_0/[Electron\ donor]_0$	Solvent	DP_{target}	Time (h)	Conv[2] (%)	k_p^{app} [3] (h^{-1})	$DP_{n,theo}$[2]	$M_{n,theo}$[4] (x10^{-3})	$M_{n,app}$[5] (x10^{-3})	M_w/M_n[5]	I_{eff}[6] (%)
1	1/0.4	1/30	DMSO	50	3.17	58.0	0.2687	29	14.6	85.9	1.58	17.0
2	1/0.4	1/30	DMAc	50	3.67	63.6	0.2778	39	16.0	85.7	1.53	18.7
3	1/0.4	1/30	DMF	50	3.67	56.7	0.2497	28	14.3	84.9	1.58	16.8
4	1/0.4	1/30	DMF	100	3	74.4	0.451	74	37.4	76.5	1.43	48.9
5	1/0.4	1/30	DMF	150	4	64.0	0.275	96	48.1	87.4	1.40	55.0
6	1/0.4	1/30	DMF	200	1.5	41.9	0.3579	83	42.0	72.8	1.37	57.7
7	1/0.4	1/30	DMF	250	2.5	47.0	0.2610	118	58.9	76.0	1.36	77.5
8	1/0.6	1/30	DMF	250	2.5	29	0.142	72	36.4	73.4	1.36	49.5

[1]General conditions: T = room temperature; V_{tot} = 5 mL; $[OEGMA_{500}]_0/[BPN]_0/[Curcumin]_0/[HMTETA]_0$ = x/1/y/z; x = 50–250; y = 0.4 for entries 1–7, and y = 0.6 for entry 8; z = 12 for entries 1–7, and z = 18 for entry 8; $[OEGMA_{500}]_0$ = 20% v/v; Blue light irradiation at 460 nm (5.0 mW cm^{-2}).
[2]Conversion and theoretical degree of polymerization ($DP_{n,theo}$) calculated according to ^{1}H NMR analysis, $DP_{n,theo}$ = (conv · $[OEGMA_{500}]_0$)/$[BPN]_0$ [55].
[3]Apparent rate constant of propagation, calculated as a slope of the curve $\ln[M]_0/[M] = f(t)$ illustrated in the Fig. 2a,c,e [21,56].
[4]$M_{n,theo}$ = $[OEGMA_{500}]_0/[BPN]_0$ · conversion · $M_{OEGMA500}$ + M_{BPN}.
[5]Apparent $M_{n,app}$ and M_w/M_n were determined by DMF GPC.
[6]Initiation efficiency, I_{eff} = ($M_{n,theo}$/ $M_{n,app}$) · 100%.

slopes are comparable for each reaction medium (see k_p^{app} in Table 2, entries 1–3). Despite the linear first-order kinetics, comparable to MMA polymerization, the rapid growth of the MWs in the initial step of the polymerization was observed, resulting in the gap between apparent MWs determined by GPC and theoretical ones. It is ascribed to the low initiation efficiency (I_{eff} ∼ 17–18%, see I_{eff} in Table 2, entries 1–3) and lagging establishment of the dynamic equilibrium between propagating radicals and dormant species. In view of the presented results, further experiments were continued in DMF.

Considering the phenomenon noted for MMA polymerization, i.e. with an increase in DP_{target}, a higher initiation efficiency was observed (Table 1, entries 7 and 8), a range of degrees of polymerization were targeted (DP_{target} = 50–250) while the ratio of initiator, curcumin and electron donor was kept constant with $[BPN]_0/[Curcumin]_0/[HMTETA]_0$ = 1/0.4/12 molar ratios in DMF. The linearity of the kinetic plots (Fig. 2c) indicated the first order relationship of the polymerizations with respect to the monomer concentration, therefore the propagating radicals kept constant during the syntheses. Usually, in accordance to the rate of polymerization (R_p) equation [57], an increase of DP_{target}, and hence the initiator concertation [PX], accelerates the reaction. Curcumin-catalyzed metal-free ATRP of $OEGMA_{500}$ in various ranges of DP_{target} did not exhibit the dependence (see k_p^{app} in Table 2, entries 3–7). The R_p value reflected by the equation is strictly connected with ATRP equilibrium constant, which is a ratio between rate constant of activation (k_{act}) and deactivation (k_{deact}) calculated for metal-based catalyst. In proposed concept a metal catalyst was substituted by organic photocatalyst. Moreover, considering the differences between molecular weights determined by GPC and theoretical ones, and rapid growth of the MWs at the initial step of the polymerization (Fig. 2d), the deactivation processes are disrupted, thus the equation does not apply in this case. It is also noted that higher DP_{target} (lower $[BPN]_0$) results in the final products with lower dispersity and higher initiation efficiency (M_w/M_n = 1.36 and I_{eff} = 77.5% for DP_{target} = 250, see M_w/M_n and I_{eff}, Table 2, entries 3–7). It can be concluded that higher monomer concentration caused faster initiator deactivation, therefore the polymer reaches the final molecular weight values approximately to the theoretical ones.

The effect of the photocatalyst concentration on curcumin-catalyzed metal-free ATRP concept has been also investigated considering two various $[BPN]_0/[Curcumin]_0/[HMTETA]_0$ = molar ratios: 1/0.4/12 and 1/0.4/18. Both polymerizations are characterized by linear plots of $\ln[M]_0/[M]$ versus time indicating characteristics of first-order reactions, and the constant concertation of propagating radicals during the syntheses (Fig. 2e). The k_p^{app} values determined from the first-order kinetics plots show a negative effect of a higher amount of photoinitiator on polymerization rate, namely higher excess of the curcumin compared to BPN slow down the polymerization, and k_p^{app} value is lower (k_p^{app} = 0.263 and 0.142 for $[BPN]_0/[Curcumin]_0/[HMTETA]_0$ = 1/0.4/12 and 1/0.4/18 molar ratios, respectively, see k_p^{app} in Table 2, entries 7 and 8). Both final polymer products were characterized by comparable dispersity, however lower photoinitiator loading provided higher initiation efficiency (M_w/M_n = 1.36 and 1.36, I_{eff} = 77.5% and 49.5% for $[BPN]_0/[Curcumin]_0/[HMTETA]_0$ = 1/0.4/12 and 1/0.4/18 molar ratios, respectively, see M_w/M_n and I_{eff} in Table 2, entries 7 and 8).

The results suggest that a higher concentration of photoinitiators causes a higher concentration of propagating radicals, and a poor deactivation process and the establishment of the dynamic equilibrium between propagating radicals and dormant species (Fig. 2f). This phenomenon leads to the formation of a high molecular weight polymer in the initial step of the polymerization and low initiation efficiency.

Curcumin-catalyzed metal-free ATRP of $OEGMA_{500}$ with the use of comestible curcumin

Curcumin is a phytochemical found in turmeric spice that comes from the root of a plant known as Curcuma Longa. Turmeric is a great source of curcumin [58]. A turmeric root typically contains ∼ 2% by weight of the root of turmeric [59]. To make the proposed approach more economical, various commercially available curcumin was used to polymerize $OEGMA_{500}$ at $[OEGMA_{500}]_0/[BPN]_0/[Curcumin]_0/[HMTETA]_0$ = 150/1/0.4/12 molar ratio in DMF (Table 3, entries 2–5), comparing them to synthesis with high-purity curcumin (Table 3, entry 1 the same as Table 2, entry 5).

Commercially-available curcumin brands APETITA, PRYMAT and KAMIS did not provide control during the polymerization. The non-linear fitting curves ($\ln[M]_0/[M]$ versus time) suggested high concentration of propagating radicals in the initial step of the polymerization (∼0.5 h for APETITA and 1.5 h – PRYMAT and KAMIS) (Fig. 3a). After that, no further conversion was detected, thus the reaction plateaued. Despite the dispersity of the final polymer products comparable to the polymers provided by laboratory curcumin-catalyzed polymerization, a low initiation efficiency was noted (I_{eff} = 11–16%, see I_{eff} in Table 3, entries 2–4). Worth mentioning that spices produced from turmeric contain ∼2% by weight of curcumin [59], therefore the syntheses were conducted with 50-fold lower curcumin loading than high-purity curcumin

Table 3
Polymerization of oligo(ethylene glycol methyl ether) methacrylate by curcumin catalyzed metal-free ATRP concept.[1]

Entry	Curcumin type	Time (h)	Conv[2] (%)	k_p^{app}[3] (h^{-1})	$DP_{n,theo}$[2]	$M_{n,theo}$[4] (x10^{-3})	$M_{n,app}$[5] (x10^{-3})	M_w/M_n[5]	I_{eff}[6] (%)
1	Pure	4	54.5	0.296	81	41.0	86.2	1.40	47.5
2	(AP) APETITA[8]	2.5	10.3	0.062	15	7.9	69.7	1.34	11.3
3	(PR) PRYMAT[8]	2.5	17.8	0.094	27	13.5	105.3	1.28	12.8
4	(KM) KAMIS[8]	2.5	25.0	0.142	37	18.9	117.0	1.27	16.1
5	(LD) LIDL[8]	2.5	42.0	0.214	63	31.7	80.7	1.35	39.0

[1]General conditions: T = room temperature; V_{tot} = 5 mL; $[OEGMA_{500}]_0/[BPN]_0/[Curcumin]_0/[HMTETA]_0$ = 150/1/0.4/12; $[OEGMA_{500}]_0$ = 20% v/v; Blue light irradiation at 460 nm (5.0 mW cm^{-2}).
[2]Conversion and theoretical degree of polymerization ($DP_{n,theo}$) calculated according to ^1H NMR analysis, $DP_{n,theo} = (conv \cdot [OEGMA_{500}]_0)/[BPN]_0$) [55].
[3]Apparent rate constant of propagation, calculated as a slope of the curve $\ln[M]_0/[M] = f(t)$ illustrated in the Fig. 3a [21,56].
[4]$M_{n,theo} = [OEGMA_{500}]_0/[BPN]_0 \cdot conversion \cdot M_{OEGMA500} + M_{BPN}$.
[5]Apparent $M_{n,app}$ and M_w/M_n were determined by DMF GPC.
[6]Initiation efficiency, $I_{eff} = (M_{n,theo}/M_{n,app}) \cdot 100\%$.
[7]Reaction results presented also in Table 2 as entry 5, kinetics results for a shorter time of polymerization presented in this table to compare the kinetics of all the reactions.
[8]Commercially available brands of kitchen spices.

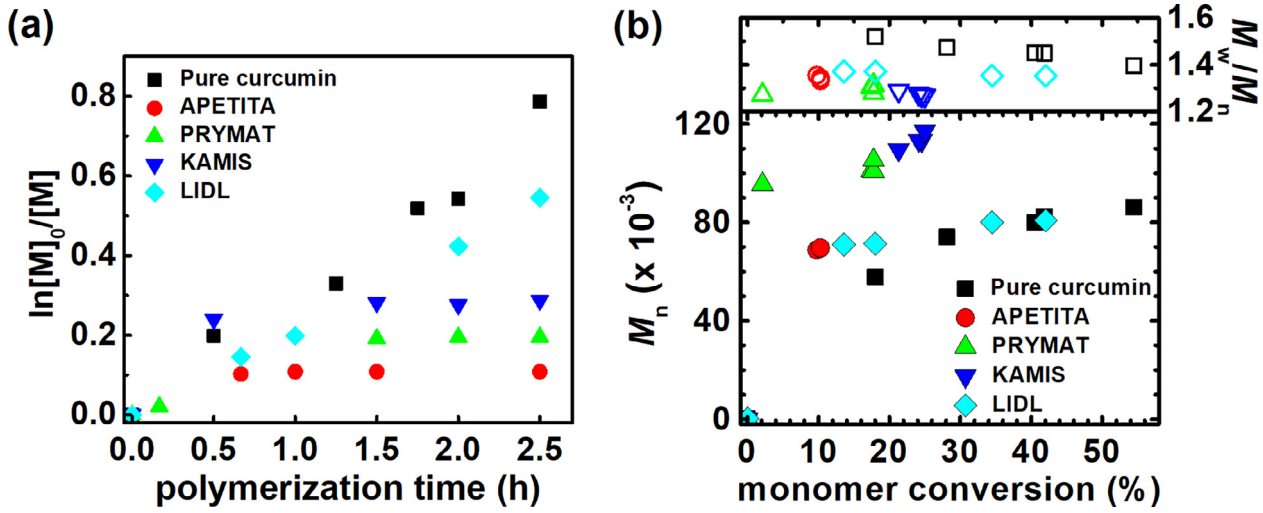

Fig. 3. The use of comestible curcumin as photocatalyst in curcumin-catalyzed metal-free ATRP of $OEGMA_{500}$: (a) first-order kinetics plot of monomer conversion vs. polymerization time, (b) M_n and M_w/M_n *vs.* monomer conversion. Table 3.

(Fig. S1). Moreover, the comestible curcumin also contains other ingredients (~98% by weight) that may interfere with the course of the polymerization.

A detailed kinetic analysis of the polymerization course with the use of commercial curcumin provided by LIDL revealed a linear increase in $\ln([M]_0/[M])$ vs. polymerization time (Fig. 3a), suggesting a constant concentration of the propagating radicals during the course of the polymerization, as the synthesis conducted with pure curcumin (Table 3, entry 5). Despite the low curcumin content in the spice, the use of the same spice mass as pure curcumin for synthesis ensured linear kinetics and high monomer conversion (conv = 42%, Table 3, entry 5), while obtaining a product with narrow molecular weight distribution (M_w/M_n = 1.35) and an initiation efficiency slightly lower than that of pure curcumin (I_{eff} = 39%). The results confirmed the successful polymerization with commercially available curcumin and suggest that other comestible curcumin ingredients, depending on the product brand, may also improve control during polymerization, even with curcumin being low in the turmeric spice.

Effect of monomer type on curcumin-catalyzed metal-free ATRP

Finally, the scope of the applicability of the proposed concept was expanded to other monomers, both methacrylates – di(ethylene glycol) methyl ether methacrylate (DEGMA), *n*-butyl methacrylate (*n*BMA) and 2-(dimethylamino)ethyl methacrylate (DMAEMA), and acrylates i.e. oligo(ethylene glycol) methyl ether acrylate ($OEGA_{480}$), 2-hydroxyethylacrylate (HEA) and *n*-butyl acrylate (*n*BA) (Table S1). The polymerizations were conducted in DMF keeping the molar ratio constant with $[Monomer]_0/[Initiator]_0/[Curcumin]_0/[HMTETA]_0$ = 300/1/0.4/12, except $OEGA_{480}$ polymerization, where DP_{target} at 150 was used. Methacrylates were polymerized from BPN initiator, while the acrylates with the use of a more suitable ATRP initiator – ethyl α-bromoisobutyrate (EBiB).

All the syntheses yielded the linear fitting curves $\ln[M]_0/[M]$ versus time reflecting first-order kinetics (Fig. S5a). Considering the methacrylates, DEGMA – another PEG-based monomer, and DMAEMA polymerization reached high monomer conversion (conv ~ 51–55%, Table S1, entries 1 and 3) and an initiation efficiency of ~40% was obtained. The controllability of the *n*BMA polymerization was rather poor with a significantly overvalued initiation efficiency (I_{eff} = 177%, Table S1, entry 2), suggesting transfer of the activity of a growing polymer chain to another molecule, and formation of short polymer chains. Only $OEGA_{480}$ among acrylate monomers exhibited the experimental molecular weight of the final product relatively agreed with the theoretical one, providing high initiation efficiency (I_{eff} = 67%, Table S1, entry 4, Fig. S5b).

Summarizing, among the monomers used, PEG-based monomers and DMAEMA show the greatest predisposition to polymerization by means of the proposed concept, while providing a

controlled polymer product with a relatively high initiation efficiency. Unexpectedly, the polymerization of acrylates was characterized by lower apparent rate constants of propagation (see k_p^{app}, Table S1), although acrylates are characterized by higher propagation rate coefficients than methacrylates [60]. However, the stability of the used initiators should be also considered in this context. Methacrylates form tertiary radicals which are more stable than a secondary radical formed by acrylates, while BPN initiator provides a secondary starting radical group, and conversely, EBiB as an initiator applied for acrylates polymerization generates more stable tertiary starting radicals. Therefore, in the proposed curcumin-catalyzed metal-free ATRP concept the methacrylates polymerize much faster. However, k_p^{app} values increase with the increasing length of the ester side chain, a trend that complies with previously observed phenomena for both groups of monomers [61].

Polymerization mechanism

Based on previous research on organo-dyes as photoredox catalysts for metal-free ATRP, the mechanism of the curcumin-catalyzed polymerization in the presence of an electron donor can be proposed. Curcumin is characterized by a reduction potential of −1.2 V [51], comparable to other successfully used dyes as photoredox catalyst i.e. fluorescein (E^*_{red} = -1.22 V [22]). Therefore, similarly to other electron-acceptor dyes i.e. eosin Y, fluoresceine or erythrosine B [22,43] it is a well-known reducible dye with a wide absorption range of visible light up to around 600 nm. Low reduction potential is one of the criteria that must be met for a photoredox catalyst to function effectively. Another advantage of curcumin, which effectively mediates photoinduced polymerization, is its low fluorescence quantum yield (Φ = 0.022–0.041 [62], hence the energy received by the dye is poorly converted to fluorescence, but is wasted on heat dissipation and other energy transfers. The proposed mechanism of the curcumin-catalyzed metal-free ATRP under visible light according to a reductive quenching cycle is shown in Scheme 1. Curcumin absorbs visible light (460 nm, 5.0 mW cm^{-2}) to afford its highly reactive excited species Cur*, which is capable of transferring an electron by photo-induced electron transfer (PET). Electron donor amines (TEA, PMDETA or HMTETA) quenched an electron from Cur* to generate a Cur radical anion ($Cur^{\bullet -}$) and an amine radical cation $Et_3N^{\bullet +}$ derived from the oxidation of an electron donor.

Photoredox catalyst is regenerated to its ground state by transferring an electron to the alkyl halide or polymer chain ends forming an electron-deficient alkyl radical or propagating radical and bromine anion. Adding a monomer causes the propagation reactions with formed radicals, and simultaneously oxidized amine participates in a single electron oxidation of bromine anion to generate bromine radical and regenerate the amine. The formed bromine radical deactivates the propagating radicals, and the cycle is repeated continually.

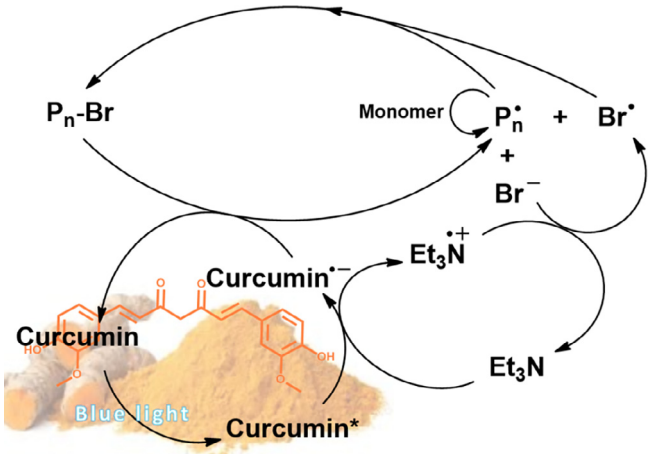

Scheme 1. Proposed mechanisms for metal-free ATRP mediated by curcumin in the presence of sacrificial electron donor, tertiary amine.

Chain extension in situ polymerization

In order to examine the chain-end fidelity of the received polymers, in situ block copolymerization experiments were successfully performed upon addition of MMA to synthesize a statistical copolymer block to a well-defined POEGMA macromonomer without purification (Table 4, Fig. S16).

The reactivity ratio of $OEGMA_{500}$/MMA was close to 2 (*r*PEGMA ∼ 1.33, *r*MMA ∼ 0.75 [63]) and statistical copolymers were expected to be obtained from in situ MMA chain extension. The PEG-based polymer was synthesized to 44.5% of monomer conversion (M_n = 91,882, M_w/M_n = 1.37), and subsequently a degassed 2 mL of MMA was injected into the reaction. Further irradiation of the reaction mixture caused an increase of the molecular weight of the polymer to 100,600 retaining narrow, monomodal molecular weight distribution as presented in Fig. 4. GPC analyses clearly showed shifts to lower retention volumes, indicating successfully conducted polymerizations from the chain ends of the precursor POEGMA.

Conclusions

In conclusion, curcumin as a reducible dye in the presence of amine and alkyl halides was successfully investigated to control metal-free ATRP concept mediated by a blue LED irradiation (λ_{max} = 460 nm, 5 mW cm^{-2}). The proposed concept has been broadly optimized to alter various parameters, i.e. effect of donor type, initiator to curcumin ratio, and curcumin to electron donor ratio on MMA polymerization, and effect of solvent type, initiator concertation and initiator to curcumin ratio on $OEGMA_{500}$ polymerization. The curcumin-catalyzed metal-free ATRP provided the final products with relatively low dispersities (M_w/M_n = 1.61 of PMMA and M_w/M_n = 1.40 of POEGMA). Most importantly, comestible curcumin found in turmeric spices has proven to be an excellent and economic replacement for laboratory curcumin. The polymerization controlled by curcumin of one of the commercially available brands was characterized by a controlled course comparable to that of laboratory purity curcumin with a low dispersity final product (M_w/M_n = 1.35). In order to extend the applicability of the proposed concept, polymerizations of other methacrylates (*n*BMA, DEGMA and DMAEMA) and various acrylates (OEGA480, *n*BA and HEA). The results indicate the high predisposition of the proposed system for polymerization of PEG-based monomers i.e. DEGMA and $OEGA_{480}$ (PDEGMA: M_w/M_n = 1.56, I_{eff} = 39.0%, POEGA: M_w/M_n = 1.32, I_{eff} = 67.4%), and also DMAEMA (M_w/M_n = 1.68, I_{eff} = 42.6%) among methacrylates. In situ chain extension experiment was successfully performed upon addition of MMA to attach a statistical copolymer block to a well-defined POEGMA macromonomer without prior purification, thus confirming chain-end fidelity of the first block. The possibility of using commercially available dyes, especially non-toxic and fully-biocompatible e.g. comestible curcumin, working in the visible range with easily available and cheap light sources like LED, contribute to the efficiency, ease of use and lower cost of controlled radical polymerization processes. Compared to other ATRP techniques, the proposed concept does not require a transition metal, reducing the number of purification steps and process costs. The

Table 4
Chain extension in situ polymerization.

Entry	[Initiator]$_0$/ [Curcumin]$_0$	[Curcumin]$_0$/ [Electron donor]$_0$	DP_{target}	Time (h)	Conv[2] (%)	k_p^{app}[3] (h^{-1})	$DP_{n,theo}$[2]	$M_{n,theo}^4$ ($x10^{-3}$)	$M_{n,app}^5$ ($x10^{-3}$)	M_w/M_n^5	I_{eff}^6 (%)
1[1]	1/0.4	1/30	150	2	44.5	0.278	66	33.5	91.9	1.37	36.5
Addition of the second monomer: 2 ml of MMA[7]											
2	1/29	1/1.2	158 of $OEGMA_{500}$ 4034 of MMA	2.25	11 of $OEGMA_{500}$ 15 of MMA[8]	-	17 of $OEGMA_{500}$	605 of MMA	160.6	1.35	160

[1]General conditions: T = room temperature; V_{tot} = 5 mL; $[OEGMA_{500}]_0/[BPN]_0/[Curcumin]_0/[HMTETA]_0$ = 150/1/0.4/12; $[OEGMA_{500}]_0$ = 20% v/v; Blue light irradiation at 460 nm (5.0 mW cm^{-2}).
[2]Conversion and theoretical degree of polymerization ($DP_{n,theo}$) calculated according to ^1H NMR analysis, $DP_{n,theo}$ = (conv · $[monomer]_0$)/$[initiator]_0$) [55].
[3]Apparent rate constant of propagation, calculated as a slope of the curve $ln[M]_0/[M] = f(t)$ illustrated in the Fig. S16a [21,56].
[4]$M_{n,theo}$ = $[monomer]_0/[initiator]_0$ · conversion · $M_{monomer}$ + $M_{initiator}$.
[5]Apparent $M_{n,app}$ and M_w/M_n were determined by DMF GPC.
[6]Initiation efficiency, I_{eff} = ($M_{n,theo}$/ $M_{n,app}$) · 100%.
[7]General conditions: T = room temperature; V_{tot} = 6 mL – calculated as 5 mL (initial reaction mixture volume) – 1 ml (the volume of withdrawn kinetics sample) + 2 ml of MMA portion; $[OEGMA_{500}]_0/[MMA]/[POEGMA]_0/[Curcumin]_0/[HMTETA]_0$ = 158/4034/1/29/36; $[OEGMA_{500}]_0$ = 6% v/v; $[MMA]_0$ = 33% v/v; Blue light irradiation at 460 nm (5.0 mW cm^{-2}).
[8]Conversion and theoretical degree of polymerization ($DP_{n,theo}$) calculated according to ^1H NMR analysis comparing the area under the signals of DMF and signals for appropriate monomers: δ (ppm) = 6.08–6.12 (1H, =C*H*–) for MMA and δ (ppm) = 6.12–6.18 (1H, =C*H*–) for $OEGMA_{500}$.

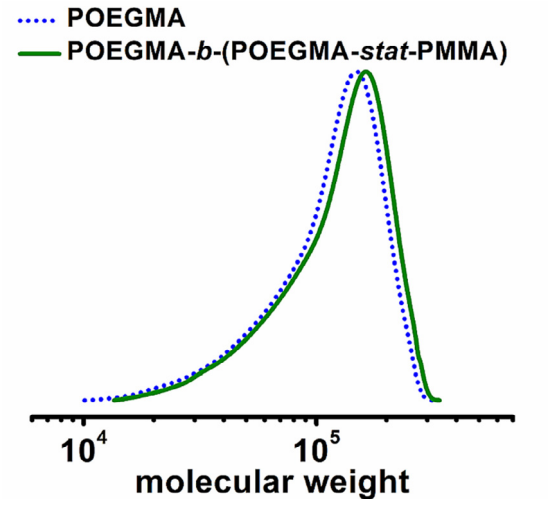

Fig. 4. GPC traces of in situ chain extension polymerization of MMA and $OEGMA_{500}$ from POEGMA first block (Table 4, entry 2).

reaction configuration is simple to use and therefore easy to adapt to the industry, only a simple LED light source is needed.

Declaration of Competing Interest

The authors declare that they have no known competing financial interests or personal relationships that could have appeared to influence the work reported in this paper.

CRediT authorship contribution statement

I. Zaborniak: Conceptualization, Methodology, Validation, Formal analysis, Investigation, Resources, Data curation, Writing – original draft, Writing – review & editing, Visualization. **P. Chmielarz:** Conceptualization, Methodology, Validation, Data curation, Writing – original draft, Writing – review & editing, Supervision, Project administration, Funding acquisition.

Declaration of Competing Interest

The authors declare that they have no known competing financial interests or personal relationships that could have appeared to influence the work reported in this paper.

Acknowledgements

Financial support from UPB.CF.20.001.01 and BK/RDKN/2020/01 is gratefully acknowledged. P.C. acknowledges Minister of Science and Higher Education scholarship for outstanding young scientists (0001/E-363/STYP/13/2018). NMR spectra were recorded in the Laboratory of Spectrometry, Faculty of Chemistry, Rzeszow University of Technology and were financed from budget of statutory activities. The Authors would like to thank Beata Motyka, MSc for photographs making to prepare graphical abstract.

Appendix A. Supplementary data

Experimental section, UV-Vis analysis of curcumin, kinetic study of polymerization, ^1H NMR and GPC analysis of synthesized polymers. Supplementary data to this article can be found online at https://doi.org/10.1016/j.jiec.2021.10.001.

References

1 N.J. Treat, H. Sprafke, J.W. Kramer, P.G. Clark, B.E. Barton, J. Read de Alaniz, B.P. Fors, C.J. Hawker, J. Am. Chem. Soc. 136 (45) (2014) 16096–16101, https://doi.org/10.1021/ja510389m.
2 G. Yilmaz, Y. Yagci, Polym. Chem. 9 (14) (2018) 1757–1762, https://doi.org/10.1039/C8PY00207J.
[3] X. Xu, X. Xu, Y. Zeng, F. Zhang, J. Photochem. Photobiol. A 411 (2021), https://doi.org/10.1016/j.jphotochem.2021.113191.
[4] Q. Ma, J. Song, X. Zhang, Y. Jiang, L. Ji, S. Liao, Nat. Commun. 12 (1) (2021) 429, https://doi.org/10.1038/s41467-020-20645-8.
5 J.S. Wang, K. Matyjaszewski, J. Am. Chem. Soc. 117 (20) (1995) 5614–5615, https://doi.org/10.1021/ja00125a035.
[6] D.J. Siegwart, J.K. Oh, K. Matyjaszewski, Prog. Polym. Sci. 37 (1) (2012) 18–37, https://doi.org/10.1016/j.progpolymsci.2011.08.001.
7 P. Chmielarz, Express Polym. Lett. 10 (10) (2016) 810, https://doi.org/10.3144/expresspolymlett.2016.76.
[8] Z. Zeng, M. Wen, G. Ye, X. Huo, F. Wu, Z. Wang, J. Yan, K. Matyjaszewski, Y. Lu, J. Chen, Chem. Mater. 29 (23) (2017) 10212–10219, https://doi.org/10.1021/acs.chemmater.7b04319.
[9] E. Trevisanello, F. De Bon, G. Daniel, F. Lorandi, C. Durante, A.A. Isse, A. Gennaro, Electrochim. Acta 285 (2018) 344–354, https://doi.org/10.1016/j.electacta.2018.07.209.
[10] M. Rolland, N.P. Truong, R. Whitfield, A. Anastasaki, ACS Macro Lett. 9 (4) (2020) 459–463, https://doi.org/10.1021/acsmacrolett.0c00121.
[11] A. Bagheri, C.M. Fellows, C. Boyer, Adv. Sci. 8 (5) (2021) 2003701, https://doi.org/10.1002/advs.202003701.
12 Y. Wang, F. Lorandi, M. Fantin, P. Chmielarz, A.A. Isse, A. Gennaro, K. Matyjaszewski, Macromolecules 50 (21) (2017) 8417–8425, https://doi.org/10.1021/acs.macromol.7b01730.
[13] N. Braidi, M. Buffagni, V. Buzzoni, F. Ghelfi, F. Parenti, M.L. Focarete, C. Gualandi, E. Bedogni, L. Bonifaci, G. Cavalca, A. Ferrando, A. Longo, I. Morandini,

N. Pettenuzzo, Macromol. Res. 29 (4) (2021) 280–288, https://doi.org/10.1007/s13233-021-9039-y.
[14] Y. Zhou, K. Wang, D. Hu, Cellulose 28 (4) (2021) 2433–2443, https://doi.org/10.1007/s10570-020-03664-y.
[15] V.A. Williams, T.G. Ribelli, P. Chmielarz, S. Park, K. Matyjaszewski, J. Am. Chem. Soc. 137 (4) (2015) 1428–1431, https://doi.org/10.1021/ja512519j.
[16] D. Konkolewicz, Y. Wang, P. Krys, M. Zhong, A.A. Isse, A. Gennaro, K. Matyjaszewski,*Polym. Chem.* **5** (15), 2014, 4396-4417, doi: 10.1039/C4PY00149D.
[17] A. Layadi, B. Kessel, W. Yan, M. Romio, N.D. Spencer, M. Zenobi-Wong, K. Matyjaszewski, E.M. Benetti, J. Am. Chem. Soc. 142 (6) (2020) 3158–3164, https://doi.org/10.1021/jacs.9b12974.
[18] J. Cuthbert, S.V. Wanasinghe, K. Matyjaszewski, D. Konkolewicz, Macromolecules 54 (18) (2021) 8331–8340, https://doi.org/10.1021/acs.macromol.1c01587.
[19] P. Chmielarz, M. Fantin, S. Park, A.A. Isse, A. Gennaro, A.J.D. Magenau, A. Sobkowiak, K. Matyjaszewski, Prog. Polym. Sci. 69 (2017) 47–78, https://doi.org/10.1016/j.progpolymsci.2017.02.005.
[20] A.A. Isse, A. Gennaro, Chem. Rec. 21 (9) (2021) 2203–2222, https://doi.org/10.1002/tcr.202100028.
[21] I. Zaborniak, P. Chmielarz, Macromol. Chem. Phys. 220 (17) (2019) 1900285, https://doi.org/10.1002/macp.201970033.
[22] J. Xu, S. Shanmugam, H.T. Duong, C. Boyer, Polym. Chem. 6 (31) (2015) 5615–5624, https://doi.org/10.1039/C4PY01317D.
[23] Y. Yang, X. Liu, G. Ye, S. Zhu, Z. Wang, X. Huo, K. Matyjaszewski, Y. Lu, J. Chen, ACS Appl. Mater. Interfaces 9 (15) (2017) 13637–13646, https://doi.org/10.1021/acsami.7b01863.
[24] N. Corrigan, J. Yeow, P. Judzewitsch, J. Xu, C. Boyer, Angew. Chem. Int. Ed. 58 (16) (2019) 5170–5189, https://doi.org/10.1002/anie.201805473.
[25] I. Zaborniak, P. Chmielarz, K. Wolski, Eur. Polym. J. 140 (2020), https://doi.org/10.1016/j.eurpolymj.2020.110055.
[26] I. Zaborniak, A. Macior, P. Chmielarz, M.C. Najarro, J. Iruthayaraj, Polymer 219 (2021), https://doi.org/10.1016/j.polymer.2021.123537.
[27] I. Zaborniak, P. Chmielarz, Eur. Polym. J. 142 (2021), https://doi.org/10.1016/j.eurpolymj.2020.110152.
[28] A. Ma, J. Zhang, N. Wang, L. Bai, H. Chen, W. Wang, H. Yang, L. Yang, Y. Niu, D. Wei, Ind. Eng. Chem. Res. 57 (51) (2018) 17417–17429, https://doi.org/10.1021/acs.iecr.8b05020.
[29] S. Beyazit, S. Ambrosini, N. Marchyk, E. Palo, V. Kale, T. Soukka, B. Tse Sum Bui, K. Haupt, *Angew. Chem. Int. Ed.* **53** (34), 2014, 8919-8923, doi: 10.1002/anie.201403576.
[30] C. Kütahya, C. Schmitz, V. Strehmel, Y. Yagci, B. Strehmel, Angew. Chem. Int. Ed. 57 (26) (2018) 7898–7902, https://doi.org/10.1002/anie.201802964.
[31] T. Zhang, T. Chen, I. Amin, R. Jordan, Polym. Chem. 5 (16) (2014) 4790–4796, https://doi.org/10.1039/C4PY00346B.
32 C. Kütahya, F.S. Aykac, G. Yilmaz, Y. Yagci, Polym. Chem. 7 (39) (2016) 6094–6098, https://doi.org/10.1039/C6PY01417H.
[33] D. Konkolewicz, K. Schröder, J. Buback, S. Bernhard, K. Matyjaszewski, ACS Macro Lett. 1 (10) (2012) 1219–1223, https://doi.org/10.1021/mz300457e.
[34] C. Kütahya, Y. Zhai, S. Li, S. Liu, J. Li, V. Strehmel, Z. Chen, B. Strehmel, Angew. Chem. Int. Ed. 60 (19) (2021) 10983–10991, https://doi.org/10.1002/anie.202015677.
[35] X. Pan, N. Malhotra, J. Zhang, K. Matyjaszewski, Macromolecules 48 (19) (2015) 6948–6954, https://doi.org/10.1021/acs.macromol.5b01815.
[36] Y. Tong, Y. Liu, Q. Chen, Y. Mo, Y. Ma, Macromolecules 54 (13) (2021) 6117–6126, https://doi.org/10.1021/acs.macromol.1c00482.
[37] G. Zhang, I.Y. Song, K.H. Ahn, T. Park, W. Choi, Macromolecules 44 (19) (2011) 7594–7599, https://doi.org/10.1021/ma201546c.
[38] L. Huang, S. Yu, W. Long, H. Huang, Y. Wen, F. Deng, M. Liu, W. Xu, X. Zhang, Y. Wei, Micropor. Mesopor. Mater. 308 (2020), https://doi.org/10.1016/j.micromeso.2020.110520.
[39] G.M. Miyake, J.C. Theriot, Macromolecules 47 (23) (2014) 8255–8261, https://doi.org/10.1021/ma502044f.
[40] S. Tan, J. Xiong, Y. Zhao, J. Liu, Z. Zhang, J. Mater. Chem. C 6 (15) (2018) 4131–4139, https://doi.org/10.1039/C8TC00781K.
[41] D.A. Corbin, K.O. Puffer, K.A. Chism, J.P. Cole, J.C. Theriot, B.G. McCarthy, B.L. Buss, C.-H. Lim, S.R. Lincoln, B.S. Newell, G.M. Miyake, Macromolecules 54 (10) (2021) 4507–4516, https://doi.org/10.1021/acs.macromol.1c00501.
[42] P. Li, Y. Zhang, P. Gong, Y. Liu, W. Feng, H. Yang, Talanta 235 (2021), https://doi.org/10.1016/j.talanta.2021.122803.
[43] X. Liu, L. Zhang, Z. Cheng, X. Zhu, Polym. Chem. 7 (3) (2016) 689–700, https://doi.org/10.1039/C5PY01765C.
[44] Y. Zhang, M. Bradley, J. Geng, Polym. Chem. 10 (35) (2019) 4769–4773, https://doi.org/10.1039/C9PY00774A10.1039/C9PY00774A.
[45] G. Noirbent, F. Dumur, Eur. Polym. J. 142 (2021), https://doi.org/10.1016/j.eurpolymj.2020.110109.
[46] Y. Huang, S. Cao, Q. Zhang, H. Zhang, Y. Fan, F. Qiu, N. Kang, Arch. Biochem. Biophys. 646 (2018) 31–37, https://doi.org/10.1016/j.abb.2018.03.030.
[47] Z. Fan, J. Li, J. Liu, H. Jiao, B. Liu, ACS Appl. Mater. Interfaces 10 (28) (2018) 23595–23604, https://doi.org/10.1021/acsami.8b06236.
[48] Z. Rafiee, M. Nejatian, M. Daeihamed, S.M. Jafari, Trends Food Sci. Technol. 88 (2019) 445–458, https://doi.org/10.1016/j.tifs.2019.04.017.
[49] J.V. Crivello, U. Bulut, J. Polym. Sci. A 43 (21) (2005) 5217–5231, https://doi.org/10.1002/pola.21017.
[50] J.V. Crivello, U. Bulut, Macromol. Symp. 240 (1) (2006) 1–11, https://doi.org/10.1002/masy.200650801.
[51] J. Zhao, J. Lalevée, H. Lu, R. MacQueen, S.H. Kable, T.W. Schmidt, M.H. Stenzel, P. Xiao, Polym. Chem. 6 (28) (2015) 5053–5061, https://doi.org/10.1039/C5PY00661A.
[52] E. Sprick, B. Graff, J.-M. Becht, T. Tigges, K. Neuhaus, C. Weber, J. Lalevée, Eur. Polym. J. 134 (2020), https://doi.org/10.1016/j.eurpolymj.2020.109794.
[53] A. Mishra, S. Daswal, J. Macromol. Sci. A 42 (12) (2005) 1667–1678, https://doi.org/10.1080/10601320500246974.
[54] A. Mishra, S. Daswal, Colloid Polym. Sci. 285 (10) (2007) 1109–1117, https://doi.org/10.1007/s00396-007-1662-4.
[55] I. Zaborniak, P. Chmielarz, M.R. Martinez, K. Wolski, Z. Wang, K. Matyjaszewski, Eur. Polym. J. 126 (2020), https://doi.org/10.1016/j.eurpolymj.2020.109566.
56 I. Zaborniak, P. Chmielarz, Express Polym. Lett. 14 (2020) 235–247, https://doi.org/10.3144/expresspolymlett.2020.20.
[57] P. Chmielarz, A. Sobkowiak, K. Matyjaszewski, Polymer 77 (2015) 266–271, https://doi.org/10.1016/j.polymer.2015.09.038.
[58] A. Masek, E. Chrzescijanska, M. Zaborski, Electrochim. Acta 107 (2013) 441–447, https://doi.org/10.1016/j.electacta.2013.06.037.
[59] A.M. Anderson, M.S. Mitchell, R.S. Mohan, J. Chem. Educ. 77 (3) (2000) 359, https://doi.org/10.1021/ed077p359.
[60] S. Beuermann, M. Buback, Prog. Polym. Sci. 27 (2) (2002) 191–254, https://doi.org/10.1016/S0079-6700(01)00049-1.
[61] A.P. Haehnel, M. Schneider-Baumann, K.U. Hiltebrandt, A.M. Misske, C. Barner-Kowollik, Macromolecules 46 (1) (2013) 15–28, https://doi.org/10.1021/ma302319z.
[62] K.I. Priyadarsini, J. Photochem. Photobiol. C 10 (2) (2009) 81–95, https://doi.org/10.1016/j.jphotochemrev.2009.05.001.
[63] I. Ydens, P. Degée, D.M. Haddleton, P. Dubois, Eur. Polym. J. 41 (10) (2005) 2255–2263, https://doi.org/10.1016/j.eurpolymj.2005.04.012.